IOPscience iopscience.iop.org

Home Search Collections Journals About Contact us My IOPscience

Chemisorption and repulsive physisorption potentials from a unified treatment

This article has been downloaded from IOPscience. Please scroll down to see the full text article.

2000 J. Phys.: Condens. Matter 12 8369

(http://iopscience.iop.org/0953-8984/12/39/302)

View the table of contents for this issue, or go to the journal homepage for more

Download details:
IP Address: 171.66.16.221
The article was downloaded on 16/05/2010 at 06:50

Please note that terms and conditions apply.

J. Phys.: Condens. Matter **12** (2000) 8369–8386. Printed in the UK PII: S0953-8984(00)12579-2

Chemisorption and repulsive physisorption potentials from a unified treatment

P G Bolcatto†‡, E C Goldberg‡§ and M C G Passeggi§‖

† Facultad de Formación Docente en Ciencias, Universidad Nacional del Litoral, Santiago del Estero 2829, 3000 Santa Fe, Argentina
‡ Facultad de Ingeniería Química, Universidad Nacional del Litoral, Sgo del Estero 2829, 3000 Santa Fe, Argentina
§ INTEC (CONICET-UNL), Guemes 3450, cc91, 3000 Santa Fe, Argentina
‖ Facultad de Bioquímica y Ciencias Biológicas, Universidad Nacional del Litoral, POB 91, 3000 Santa Fe, Argentina

Received 14 March 2000, in final form 28 June 2000

Abstract. By using an extended Anderson's model Hamiltonian free from adjustable parameters, and where the atom–surface interaction system is built from the basic dimeric components, we show that the short-range contribution to the interaction energy provides a unified basis for describing chemisorption and the repulsive part of the physisorption potential. Using this, we analyse the process of chemisorption of H on Al and Li surfaces by examining a variety of crystalline faces and adsorption sites. The results are in good agreement with those obtained by different theoretical methods and also with the available experimental data. This model calculation is also applied to investigate the interaction of He with Al and Na surfaces. We calculate the repulsive contribution to the interaction energy covering five orders of magnitude on the energy scale. We find that it shows a Molliere-like dependence with increasing adsorbate–substrate separations. Also, we have verified that the differences in the physisorption potentials introduced by selecting different van der Waals attractive potentials may even be much larger than those caused by the differences in modelling of the repulsive potentials.

1. Introduction

The theoretical descriptions of systems consisting of atoms or molecules interacting with solid surfaces have been produced by using a variety of basic pictures that tend to emphasize different aspects of the mechanisms relevant to these processes. The diversity of the theoretical approaches arises naturally because of the intrinsic complexity of the problem. In this work we will concentrate on just two of the possible phenomena: the chemical and physical adsorption of a single atom on a metal surface. There is no clear-cut way to distinguish between these two kinds of process, although one refers to chemisorption when the adsorbed species (adatom) reacts chemically with the substrate, transferring charge, with binding energies typically around 2–3 eV and equilibrium distances from the surface of the order of 3 au. At the other extreme, for non-reactive adatoms (such as noble-gas atoms) where, thanks to the van der Waals interaction the energy can have a shallow minimum of about 10 meV at distances $\sim$10 au, one speaks of physisorption. The wide ranges of the binding energies and distances involved in the description of the atom–surface interaction require a detailed balance of all the contributions to the basic potential terms. Thus, calculations that allow for a description of the adsorption process covering the entire range represent a very hard task. Therefore, different theoretical

0953-8984/00/398369+18$30.00 © 2000 IOP Publishing Ltd

approaches have been proposed depending on the distances of interest [1]. The energy of interaction between the adatom and the substrate can be defined as the difference of the average of the Hamiltonian for a given atom–surface distance R and the corresponding average when the subsystems are infinitely far apart. Although it is not rigorous, this interaction energy is usually thought to arise from two kinds of contribution: one part that takes into account the effects of short-range interactions due to the overlap between the electron clouds of the atom and the metal, and the remaining one that includes the long-range (attractive) polarization potential effects [2]:

$$E_{int} = \langle H \rangle_R - \langle H \rangle_\infty = V_{SR}(R) + V_{LR}(R). \tag{1}$$

For chemisorption, all the equilibrium properties are fairly well described by the short-range contribution $V_{SR}(R)$. Most of the successful chemisorption calculations have been performed within density functional theory [3] (DFT) using the local spin-density approximation [4] (LSDA) and the generalized gradient approximation [5] (GGA). In many cases, it is possible to verify that correlation effects are less important than exchange contributions, and consequently that these latter are the ones that should be considered carefully [2]. The non-locality of the exchange part of the electron–electron interaction can be accounted for at least partially within the Hartree–Fock (HF) approximation, and this may be sufficient when dealing with chemisorption problems. Thus, as chemisorption is considered a localized process, $V_{SR}(R)$ usually contains all the attractive and repulsive ingredients required to describe these situations. An alternative to DFT is provided by the methods based on the cluster approach [6–8]. These molecular physics schemes tend to produce results that are strongly dependent on the cluster size, although several embedding techniques have been developed to avoid this undesirable effect [9–11].

By contrast, when inert adatoms are considered, $V_{LR}(R)$ in equation (1) becomes essential because it provides the only attractive contribution in the description of the physisorption, since in these cases $V_{SR}(R)$ is always repulsive. In fact, $V_{LR}(R)$ is the van der Waals potential and its calculation involves the computation of the dielectric response function, implying a problem with a non-trivial resolution. Zaremba and Kohn (ZK) [2] proposed an approximation in which the mutually induced long-range contribution to the energy was calculated in terms of the frequency-dependent atomic polarizability and the dielectric function for the isolated substrate. This scheme has been revisited on an *ab initio* basis [12–14], and although excellent results for atom–atom interactions were obtained [14], the atom–metal interaction system still remains an open problem. The calculation of $V_{SR}(R)$ also represents a difficult task in itself. Effective theories [15] interpret this potential as being directly proportional to the unperturbed electronic density of the solid. The experimental evidence of anticorrugation [16] (i.e. closer-than-expected approach of the projectiles to the surface in regions with high electronic density) alert us to potential problems with adopting such simplifying assumptions, which may become unreliable, and to the fact that major theoretical efforts are required [17]. ZK [2] have emphasized the importance of the hybridizations due to the overlap between the wave functions of the adatom and the surface states in defining $V_{SR}(R)$. Subsequent works [18, 19] have also pointed in the same direction, although where physisorption potentials are concerned, only asymptotic expressions have been given.

In a previous work, we have presented an extended version of the Anderson model [20] to describe the atom–surface interaction within a single-particle approximation without requiring the use of semi-empirical parameters. The on-site energy and hopping parameters were calculated in terms of both the local density of states of the surface and the atomic states (including some selected one- and two-electron interactions). Thus, the extended nature of the surface states and the localized features of the atom–atom interactions are preserved on

an *ab initio* basis. In a first stage, the model was applied to the study of some examples of chemisorbed H/metal systems and also applied as a prescription for obtaining distance-dependent parameters required to deal with dynamic processes involving charge exchange. In the present paper, we report new results obtained after applying the same procedure based on our model Hamiltonian to the chemisorption of H on Li, Al for different local arrangements of the adsorbate–substrate system as well as results for the repulsive (short-range-effects) contribution to the physisorption potential of He–Al and He–Na. In the latter case, as the model does not include long-range effects caused by electron correlations, the description of the adsorbate–surface system at intermediate and long separation distances ($z \gtrsim$ 4–5 au) is limited to considering the repulsive part of the potential, while the attractive (van der Waals) contribution is added separately.

In section 2 a summary of the theoretical steps leading to the building of the single-particle Hamiltonian is given as well as the procedure followed to calculate the interaction energy. The results obtained for the H adsorption on different metal faces (Li, Al) and sites are discussed and compared with those from other authors in section 3. Also, the repulsive contributions to the physisorption potential of He–Al and He–Na and the possibility of including long-range interaction effects to account for correlation effects at the surface are examined and the results compared with other existing results. Conclusions are given in section 4.

2. Theory

2.1. Short-range potentials $V_{SR}(z)$

The short-range potential $V_{SR}(z)$ can be obtained as the difference between the average of an effective (HF) Hamiltonian for a given atom–surface separation z and the corresponding average for the situation where the subsystems are infinitely far apart:

$$V_{SR}(z) = \langle H^{HF} \rangle_z - \langle H^{HF} \rangle_\infty. \tag{2}$$

To obtain $V_{SR}(z)$ according to equation (2), we use the previously developed bond-pair model Hamiltonian. Details of this model have been given previously [20] and will be omitted here. As our starting point, we take the effective one-particle Hamiltonian that looks exactly the same as an extended HF version of the Anderson Hamiltonian:

$$\begin{aligned} H^{HF} &= H^{ads} + H^{sub} + H^{int} + V_{n-n} - [\mathrm{X}] \\ &= \sum_{\alpha\sigma} E_\alpha^\sigma \hat{n}_{\alpha\sigma} + \sum_{\boldsymbol{k}\sigma} E_{\boldsymbol{k}}^\sigma \hat{n}_{\boldsymbol{k}\sigma} + \sum_{\boldsymbol{k}\alpha\sigma} [(T_{\alpha\boldsymbol{k}}^\sigma - G_{\alpha\boldsymbol{k}} \langle c_{\boldsymbol{k}\sigma}^\dagger c_{\alpha\sigma} \rangle) \hat{c}_{\alpha\sigma}^\dagger \hat{c}_{\boldsymbol{k}\sigma} + \mathrm{H.c.}] \\ &\quad + V_{n-n} - [\mathrm{X}] \end{aligned} \tag{3}$$

where we have added the nuclear repulsion term V_{n-n} and the double-counted terms to be subtracted after performing the HF approximation (symbolized as [X]) in order to allow for a correct calculation of the interaction energy. In the traditional form of the Anderson Hamiltonian, although both the adsorbate $|\alpha\rangle$ (or the 'impurity') and the set of $|\boldsymbol{k}\rangle$ ('band') states are assumed mutually orthonormal, the accompanying parameters E_α^σ and $E_{\boldsymbol{k}}^\sigma$ are taken as those corresponding to the isolated adsorbate and substrate subsystems. In our extended version, all the states form an orthonormal basis set, and then $|\alpha\rangle$ and $|\boldsymbol{k}\rangle$ at finite adatom–surface separation distances do not correspond to eigenstates of any of the two isolated subsystems. Since a complete orthogonalization of the two sets of states is out of the question, all parameters in equation (3) finally involve an expansion of all matrix elements in terms of the overlap matrix elements $S_{\alpha\boldsymbol{k}}$. Thus, an energy parameter such as E_α includes the energy level of the isolated atom, the one-electron Coulomb attraction of the nuclei of the substrate (crystal-field terms), the two-electron Coulomb repulsion (on-site and intersite), and correction terms proportional

to overlaps such as $-ST$ and $S^2(E_\alpha - E_{\boldsymbol{k}})/4$, resulting from the orthogonalization procedure. The main differences from the standard Anderson model are:

(i) The adsorbate–substrate two-electron interactions are explicitly considered within the mean-field approximation.
(ii) The whole adsorbate and the substrate levels are modified by the orthogonalization effects.
(iii) H^{sub} includes the inner energy bands.
(iv) The hopping term in equation (3) results from the addition of two contributions: $T^\sigma_{\alpha\boldsymbol{k}}$ which is the standard hopping between orthogonalized functions†, and $-G_{\alpha\boldsymbol{k}}\langle c^\dagger_{\boldsymbol{k}\sigma}c_{\alpha\sigma}\rangle$ which accounts for the correct non-locality of the exchange interaction within the mean-field description.

Actually, E^σ_α and $E^\sigma_{\boldsymbol{k}}$ (as $T^\sigma_{\alpha\boldsymbol{k}}$) depend on the occupation numbers associated with the localized states with spin index σ, $\langle n_{\alpha\sigma}\rangle$ for the adsorbate and $\langle n_{i\sigma}\rangle$ for the substrate, respectively‡. Averages such as $\langle n_{i\sigma}\rangle$ are obtained by integrating the local and partial densities of states corresponding to the isolated solid (assumed as δ-like forms for the inner states and semi-elliptical functions for the valence bands). On the other hand, $\langle n_{\alpha\sigma}\rangle$ and $\langle c^\dagger_{\alpha\sigma}c_{i\sigma}\rangle$ are calculated self-consistently using standard Green's function techniques. From the chemisorption function $\Delta^\sigma(\varepsilon)$ (the imaginary part of the Green's function) and its Hilbert transform $\Lambda^\sigma(\varepsilon)$ (the real part of the Green's function), the occupation number $\langle n_{\alpha\sigma}\rangle$ is given by

$$\langle n_{\alpha\sigma}\rangle = -\frac{1}{\pi}\sum_{i\boldsymbol{R}_s}\int_{\varepsilon_{bi}}^{\varepsilon_f}\frac{\rho^\sigma_{i\boldsymbol{R}_s}(\varepsilon)|T^\sigma_{\alpha i} - G_{\alpha i}\langle c^\dagger_{i\sigma}c_{\alpha\sigma}\rangle|^2}{[\varepsilon - E^\sigma_\alpha - \Lambda^\sigma(\varepsilon)]^2 + [\Delta^\sigma(\varepsilon)]^2}\,\mathrm{d}\varepsilon \tag{4}$$

where $\rho^\sigma_{i\boldsymbol{R}_s}(\varepsilon)$ is the partial and local density of states corresponding to a valence state i centred at the $\boldsymbol{R}_s$-site of the solid. Also, ε_f is the Fermi level and ε_{bi} is the bottom of the valence sub-band i. Equation (4) is valid when E^σ_α is resonant with the valence band (virtual state). The corresponding expression when the denominator in (4) has a simple pole at $\varepsilon = \varepsilon_l$ (i.e. $\Lambda^\sigma(\varepsilon) = \varepsilon - E^\sigma_\alpha$ and $\Delta^\sigma(\varepsilon) = 0$), which is associated with a localized state, is

$$\langle n_{\alpha\sigma}\rangle_l = \left[1 - \Lambda'^\sigma(\varepsilon_l)\right]^{-1} \tag{5}$$

where $\Lambda'^\sigma(\varepsilon_l) = (\mathrm{d}\Lambda^\sigma(\varepsilon)/\mathrm{d}\varepsilon)|_{\varepsilon=\varepsilon_l}$. Similarly, averages of the type $\langle c^\dagger_{\alpha\sigma}c_{i\sigma}\rangle$ are obtained from the following recurrence relationship:

$$\langle c^\dagger_{\alpha\sigma}c_{i\sigma}\rangle^{out} = (T^\sigma_{\alpha i} - G_{\alpha i}\langle c^\dagger_{i\sigma}c_{\alpha\sigma}\rangle^{in})\int_{\varepsilon_{bi}}^{\varepsilon_f}\frac{\rho^\sigma_{i\boldsymbol{R}_s}(\varepsilon)(\varepsilon - E^\sigma_\alpha)}{[\varepsilon - E^\sigma_\alpha - \Lambda^\sigma(\varepsilon)]^2 + [\Delta^\sigma(\varepsilon)]^2}\,\mathrm{d}\varepsilon \tag{6}$$

for E^σ_α resonant with the valence band, while

$$\langle c^\dagger_{\alpha\sigma}c_{i\sigma}\rangle^{out}_l = \frac{\Lambda^\sigma_i(\varepsilon_l)}{(T^\sigma_{\alpha i} - G_{\alpha i}\langle c^\dagger_{i\sigma}c_{\alpha\sigma}\rangle^{in})[1 - \Lambda^{\sigma\prime}(\varepsilon_l)]} \tag{7}$$

when localized states appear.

† It can be shown that in order to obtain results that are physically correct, the functions that define the hopping term must be orthogonal. This is possible only if an approximation is performed over the three-centre integrals, so as to decompose the hopping into a sum of hopping pairs. Thus, the complete system can then be built starting from the elemental dimers. See the details in references [20] and [26].

‡ The self-consistent procedure is carried out after performing an LCAO expansion of the $|\boldsymbol{k}\rangle$ states. In consequence, self-consistency is achieved in terms of averages such as $\langle n_{i\sigma}\rangle$ and $\langle c^\dagger_{i\sigma}c_{\alpha\sigma}\rangle$ (where i includes all labels referring to the states of a given site in the substrate), instead of the starting averages $\langle n_{\boldsymbol{k}\sigma}\rangle$ and $\langle c^\dagger_{\boldsymbol{k}\alpha}c_{\alpha\sigma}\rangle$.

2.2. Long-range potentials $V_{LR}(z)$

As mentioned previously, the long-range attractive contribution to the interaction energy for the physisorption problem can be approximated through a van der Waals potential. For distances far from the surface, this potential is given by

$$V_{LR}(z) \equiv V_{vdW}(z) = -\frac{C_3}{(z - Z_{vdW})^3} + \mathrm{O}(z - Z_{vdW})^{-5} \tag{8}$$

where the parameters C_3 and Z_{vdW} are related to the polarizability of the adsorbate and to the dielectric function of the solid. The calculation of the correction terms $\mathrm{O}(z - Z_{vdW})^{-5}$ is a very hard task, and in general only the first term of equation (8) is used to approximate the van der Waals interaction. However, this term diverges at $z = Z_{vdW}$ and, since $V_{SR}(z)$ is always finite, the interaction energy diverges as well. This undesirable result can be avoided if the approximated V_{vdW}-potential is multiplied by a semi-empirical function that cancels out the divergence at $z = Z_{vdW}$, preserving the form of equation (8) in the asymptotic region [18]:

$$V_{vdW} = -\frac{C_3}{(z - Z_{vdW})^3} f(z - Z_{vdW}) \tag{9}$$

where

$$f(x) = 1 - [2x(1 + x) + 1]\exp(-2x).$$

The explicit calculation of this potential is beyond the scope of this work and we will use known results to this purpose. In table 1 we summarize the values adopted for C_3 and Z_{vdW} corresponding to Al and Na surfaces. As the expression (8) is consistent with an origin of coordinates taken at the jellium edge, while $V_{SR}(z)$ is referred to the plane defined by the surface ions, the distances between the jellium edge and this plane for several crystalline faces are also included.

Table 1. C_3- and Z_{vdW}-parameters for Al and Na. We also include the distance Z_{je} between the jellium edge and the first plane of superficial ions. The unit of energy is eV and the distances are in au.

	Al		Na	
	C_3	Z_{vdW}	C_3	Z_{vdW}
ZK[a]	1.365	1.03	0.621	0.73
ZKL[b]	1.361	0.74	0.612	0.59
HAL[c]	1.769	0.77	0.844	0.53
Z_{je}	1.91 (100) 2.21 (111)		2.02 (100) 2.86 (110)	

[a] Reference [2].
[b] C_3: reference [2]; Z_{vdW}: reference [27].
[c] Reference [13].

3. Results and discussion

All the results to be presented hereafter have been obtained by using equation (1) with V_{SR} defined by equations (2) and (3), while V_{LR} is taken as in equation (9). The long-range contribution is taken into consideration only with the purpose of exhibiting the complete form of the physisorption potentials. Although the details of the calculation procedure have already been given in reference [20] and are omitted here, it is worth mentioning that the computation requirements for constructing any of the interaction energy curves are modest. They usually take a few minutes of CPU time on a medium-speed personal computer.

3.1. Chemisorption of H on Al and Li

The procedure described in the previous section has been applied to the H/Li and H/Al systems. On-top, on-bridge, and on-centre adsorption sites for Li(100), Al(100), Al(110), and Al(111) faces were examined. For Li only, s-like valence and inner bands are included, while for Al, s- and p-like valence and core bands are considered. In our simplified description, the sp-band states are assumed to be non-hybridized. The absorption of H on these metals has been studied by other authors using different theoretical approaches. These include ones based on extended models for the substrate within the DFT (at either the LSDA or the GGA level of approximation) [21, 22], as well as those involving cluster-like or embedded-cluster pictures of the solid [6–11].

3.1.1. H/Al. The interaction energies for the on-top, on-bridge, and on-centre adsorption sites for (111), (100), and (110) crystallographic faces are shown in figures 1, 2, and 3 respectively. The binding energies E_b ($E_b = -D_0$, where D_0 is the minimum of the interaction energy), equilibrium distances R_e, and vibrational frequencies ω_e are presented in tables 2, 3, and 4. The calculational findings with which we compare our results are those obtained by Hjelmberg [21] within the LSDA, by Stumpf [22] who includes GGA corrections, and by García-Vidal *et al* (GV) [23].

As regards H/Al(111) (figure 1), we found that all the curves have a correct asymptotic limit ($z \to \infty$) as well as a marked repulsive barrier for small atom–surface distances. Although aluminium is usually visualized as an electron gas of high density, the presence of a clear

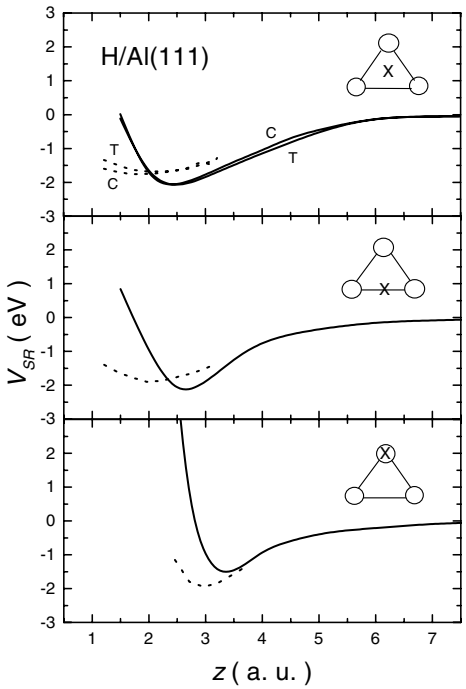

Figure 1. Interaction energy as a function of the distance between the adsorbate and the first plane of surface atoms for the H/Al(111) case. Top panel: H at the on-centre position. T (C) means that there is (is not) an atom of Al of the second superficial plane under H. Middle panel: the on-bridge position for H. Bottom panel: the on-top position for H. ——: present work; · · · · · ·: reference [21].

repulsive barrier is a signature of the localized nature of the atom–surface interaction for this system. This conclusion cannot be readily extracted from the LSDA and GV results, which present interaction curves with less structure. Our model basically represents a molecular orbital approach, because of the LCAO expansion of the $\boldsymbol{k}$-states. Thus, following this line of reasoning, one might think that a strong repulsive barrier at smaller distances is an obvious consequence of the nuclear repulsion arising from a molecular-like model. However, as we will see below, the interaction curve does not always become repulsive at short distances, and then the repulsive barrier is appropriate for this particular system.

The results for the vibrational frequencies ω_e support the previous analysis. These quantities were calculated by performing the harmonic approximation around R_e. For all of the surface faces analysed, we have found that $\omega_e^{top} > \omega_e^{bridge} > \omega_e^{centre}$, which is in agreement with the LSDA results (see table 2). Simplifying the analysis, it is possible to assume that the equilibrium properties of a chemisorbed system emerge from the balance of two competitive effects: the electronic repulsion between the electronic densities of each subsystem, and the Coulombic attraction between the electrons of the adsorbate and the nuclei of the substrate. If the former becomes the dominant interaction, the adsorbate will 'see' the solid as some sort of jellium, and the vibrational frequencies should be practically independent of the adsorption site. In contrast, if the Coulomb attraction dominates, a marked dependence on the adsorption site would be expected. Taking into account that as the adsorbate goes away from the surface, atom–atom distances vary more slowly in the on-centre case than for the on-bridge site (and, obviously, than for the on-top site), it turns out that the expected sequence should be $\omega_e^{top} > \omega_e^{bridge} > \omega_e^{centre}$. The calculations are in line with this reasoning, providing new evidence for the localized nature of the interactions.

Table 2. Binding energies E_B (eV), equilibrium distances R_e (au), and vibrational frequencies ω_e (meV) for H/Al(111). The reference data were extracted from references [21] (LSDA) and [22] (GGA).

		E_B (eV)	R_e (au)	ω_e (meV)
Top	This work	1.5	3.4	260
	LSDA	1.9	2.9	300
Bridge	This work	1.8	2.7	169
	LSDA	1.9	2.0	150
	GGA ($\Theta = 0.5$ ML)	1.96		
Centre (T)	This work	1.6	2.6	161
	LSDA	1.7	2.1	120
	GGA ($\Theta = 0.5$ ML)	1.92		
Centre (C)	This work	1.6	2.6	161
	LSDA	1.8	1.9	120
	GGA ($\Theta = 0.5$ ML)	1.99		
	GGA ($\Theta \ll 1$ ML)	1.89		

The calculated E_B are also in good agreement with LSDA and GGA ones, the largest difference being $\simeq$0.3 eV†.

The interaction energy curves for hydrogen on the (100) face of aluminium present two qualitatively different behaviours depending on the nearest-neighbour distances (figure 2).

† Table 4, later, verifies that there is an unexpected tendency of LSDA binding energies as compared with GGA values. In contrast to the case for the (100) and (110) faces, here the LSDA values are systematically smaller than GGA ones. A possible reason for this discrepancy might be that an approximated method based on pseudopotentials was used to include crystal effects.

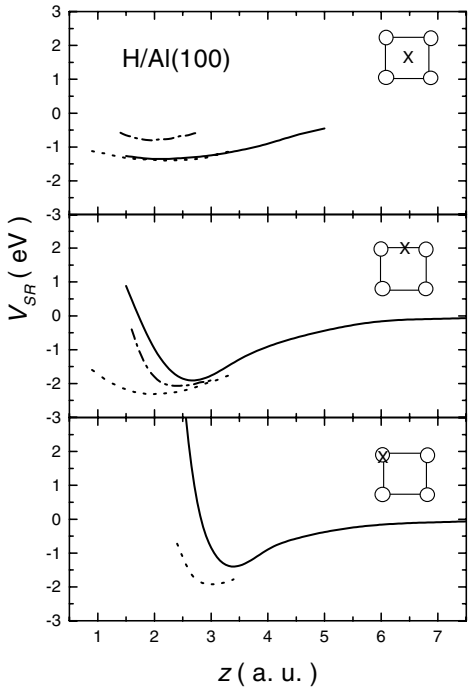

Figure 2. Interaction energy as a function of the distance between the adsorbate and the first plane of surface atoms for the H/Al(100) case. Top panel: H at the on-centre position. Middle panel: the on-bridge position for H. Bottom panel: the on-top position for H. ——: present work; · · · · · ·: reference [21]; — · —: reference [23].

Table 3. Binding energies E_B (eV), equilibrium distances R_e (au), and vibrational frequencies ω_e (meV) for H/Al(100). The reference data were extracted from references [21] (LSDA), [23] (GV), and [22] (GGA).

		E_B (eV)	R_e (au)	ω_e (meV)
Top	This work	1.5	3.4	199
	LSDA	1.9	3.0	210
Bridge	This work	2.0	2.6	167
	LSDA	2.3	2.0	130
	GGA ($\Theta = 1$ ML)	2.13		
	GGA ($\Theta \ll 1$ ML)	2.09		
	GV	2.07	2.4	
Centre	This work	1.4	2.2	68
	LSDA	1.4	2.4	70
	GV	0.8	2.0	

While for the on-top and on-bridge sites the curves look very similar to the H/Al(111) case, the interaction curve for the on-centre situation does not present a repulsive barrier. In view of the analysis in the previous paragraph, this is not an unexpected result: the on-centre site has greater nearest-neighbour distances and any effect due to direct atom–atom interactions will be diminished. Thus, the hydrogen interacts with an almost homogeneous electron gas and the repulsive barrier is expected to appear at smaller distances from the surface.

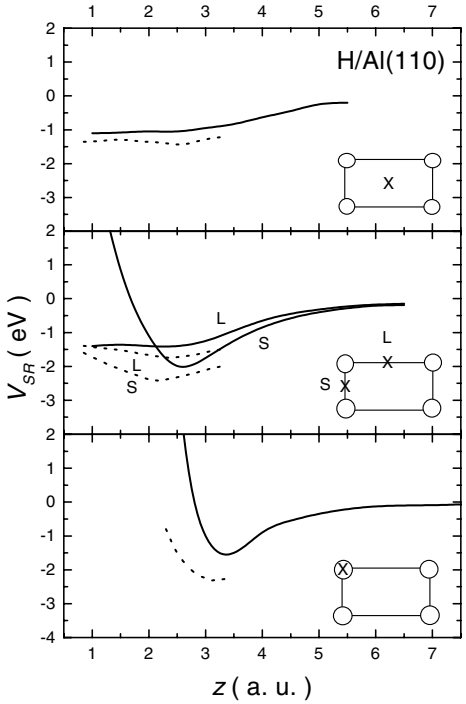

Figure 3. Interaction energy as a function of the distance between the adsorbate and the first plane of surface atoms for the H/Al(110) case. The same conventions apply as for figure 1.

Table 4. Binding energies E_B (eV), equilibrium distances R_e (au), and vibrational frequencies ω_e (meV) for H/Al(110). The reference data were extracted from references [21] (LSDA), and [22] (GGA).

		E_B (eV)	R_e (au)	ω_e (meV)
Top	This work	1.6	3.4	202
	LSDA	2.3	3.2	180
	GGA ($\Theta = 1$ ML)	2.05		
	GGA ($\Theta \ll 1$ ML)	2.09		
Bridge (S)	This work	2.0	2.6	167
	LSDA	2.4	2.2	170
	GGA ($\Theta = 1$ ML)	2.06		
Bridge (L)	This work	1.4	(2.4)	
	LSDA	1.7	2.3	110
Centre	This work	(1.1)		
	LSDA	(1.4)		

From table 3, the vibrational frequency values 199, 167, and 68 meV for on-top, on-bridge, and on-centre sites, respectively, can be compared with the experimental data from electron energy-loss spectroscopy (EELS) [24]. In the EELS spectrum, one can identify three peaks at 212 meV (1710 cm^{-1}), 164 meV (1325 cm^{-1}), and 139 meV (1125 cm^{-1}), the latter peak being the highest. The sample had a coverage of $\Theta = 0.18$ ML and the measurements were performed at temperatures lower than 90 K. On the basis of the LSDA results, the

peak at 139 meV was associated with a H twofold coordinate. Our results are in fairly good agreement with this identification, although the coincidence of ω_e^{top} and ω_e^{bridge} with two of the experimental peaks (212 meV and 164 meV, respectively) could be indicating that the actual adsorption site (identified by the peak at 139 meV) is at an intermediate location between the on-bridge and on-centre ones. All of the theoretical calculations have not included this possibility in the analysis.

Experimental data on the binding energies (for example, from thermal desorption spectroscopy) are not available for this system since, as the temperature is increased, H atoms are recombined as H_2 and then desorbed as molecules [24]. Comparison among the theoretical calculations shows that our results for E_b are in good agreement with LSDA and GGA ones. We found that the on-bridge adsorption site is the most stable, with an energy of 2.0 eV. The GGA binding energy is 2.13 eV when the coverage $\Theta = 1$ ML but with a tendency to decrease to 2.07 eV for $\Theta < 1$ ML [22]. Therefore our results differ from the GGA ones by less than 5% at low coverages. As expected, the LSDA binding energy is up to 25% greater than the GGA one. We have found better agreement with GV for the on-bridge site than for the on-centre one. This may be attributed to the fraction of the adsorbate monolayer that they were compelled to consider in the numerical calculation. For the on-centre case, the repulsion among the hydrogen electron clouds becomes more important, since adsorbate–substrate distances become larger, and therefore the binding energy will decrease. As regards the transferred charge, our results predict a charge excess on the hydrogen of 0.05, 0.05, and 0.01 electrons for the on-centre, on-bridge, and on-top adsorption sites, respectively. These results are also in agreement with the values reported by GV (0.05 for the on-bridge site).

For H/Al(110), the analysis is similar to that for the H/Al(100) case: when we consider the on-top and on-(short-)bridge sites, we obtain results very close to those for the H/Al(100) system (see figure 3 and table 4), and for the on-(long-)bridge and on-centre adsorption sites, the interaction curves do not present a repulsive barrier. As in the H/Al(100) example, the LSDA binding energies are larger than the GGA ones. Our results for the interaction energy are in good agreement with the LSDA ones, although for the on-top site our results show a more pronounced repulsion at smaller distances from the surface, producing a lower binding energy.

3.1.2. H/Li. The adsorption of hydrogen by a Li surface has been treated on the basis of a cluster description of the Li surface by Beckman and Koutecky (BK) [6] and by Hira and Ray (HR) [7]. These works consider clusters of up to ten Li atoms, involving unrestricted HF calculations corrected by correlation effects. As the convergence with respect to the number of atoms in the cluster was not properly achieved, alternatives have been proposed by Casassa and Pisani (CP) [9] based on an embedded-cluster model within a restricted HF approximation, and by Krüger and Rösch [10], who employ the moderately large-embedded-cluster (MLEC) formalism. This system has also been studied within the local density functional framework by Birkenheuer *et al* [11] using the FILMS code [25].

In table 5 our results for the binding energies, equilibrium distances, and charge transfer to the hydrogen atom are compared for on-centre adsorption sites. One can observe how the BK and HR calculations greatly depend on the size of the cluster considered. The differences in sign of the corrections due to correlation effects are indicative of the instabilities associated with the small-cluster description. The binding energy obtained with our bond-pair Hamiltonian (2.4 eV) is in good agreement with the HF values obtained by BK and HR (2.2 eV). It can also be observed that their results tend to ours as the size of the cluster is increased. The CP binding energy (3.6 eV) shows the largest discrepancy with respect to our results, and these differences can be attributed to the embedding technique used in the CP calculation. The

Table 5. Binding energies E_B (eV), equilibrium distances R_e (au), and charge transfers Δn for the on-centre site in the H/Li(100) system. The reference data were extracted from references [9] (CP), [6] (BK), [7] (HR), [10] (MLEC), [23] (GV), and [11] (FILMS). In the work of CP, BK, and HR, the numbers of Li atoms in the first, second, and third crystalline planes used in the definition of the cluster are indicated. For CP, *Sn* denotes the number of slabs of the crystalline substrate. Values in parentheses in the binding energy column correspond to a calculation including correlation effects.

On centre		E_B (eV)	R_e (au)	Δn
	This work	2.4	0.3	−0.21
	GV	2.0	−0.5	−0.60
Cluster methods	BK (4, 0)	1.7 (1.4)	0.0	—
	(4, 5)	2.2 (2.7)	0.5	—
	HR (4, 0)	1.9 (2.0)	0.45	−0.44
	(4, 5)	2.2 (3.0)	0.5	−0.36
Embedded-cluster	CP (4, 1, 4) *S*3	3.3	0.0	−0.46
methods	(4, 1, 4) *S*5	3.6	0.0	−0.46
	MLEC Li_{26}	2.48	0.34	−0.12
	Li_{30}	2.32	0.34	−0.22
	FILMS $\Theta = 1$ ML	2.99	0.25	−0.31
	$\Theta = \frac{1}{2}$ ML	2.90	0.28	−0.28

value obtained by GV (2.0 eV) is smaller than ours, and this can be understood (as in the H/Al(100) on-centre case) by taking into account the effects of repulsion between adsorbates. The comparison with FILMS results at low coverage (2.90 eV) shows that these become similar to ours (this is also true for the other properties). Good agreement is also found with MLEC results (2.32 eV).

As regards equilibrium distances, all the calculations predict a small value (in the range -0.5 au $\leqslant R_e \leqslant 0.5$ au), which is indicative of the open crystalline structure of bcc Li. Better agreement is found with MLEC and FILMS values. The charge transfers calculated by CP, BK, and HR are not strictly comparable with ours, since they employ the Mulliken population analysis in their calculations, although all agree in predicting that hydrogen acts as a charge acceptor ($\Delta n < 0$). The same tendency emerges from MLEC and FILMS predictions.

In tables 6 and 7 we present the results for on-bridge and on-top adsorption sites. As regards binding energies, we found the sequence $E_B^{on-centre} > E_B^{on-bridge} > E_B^{on-top}$. The comparison with other methods turns out to be quite difficult, because of the noticeable changes in E_B when the cluster size is increased or the correlation effects are included.

Table 6. Binding energies E_B (eV), equilibrium distances R_e (au), and charge transfers Δn for the on-bridge site in the H/Li(100) system. The same conventions apply as for table 5.

On bridge		E_B (eV)	R_e (au)	Δn
	This work	2.2	(−0.9)	−0.27
Cluster methods	BK (2, 2)	2.29 (2.04)	−1.65	—
	(6, 2)	2.69 (2.97)	−2.50	—
	HR (2, 2)	1.55 (1.85)	−1.60	−0.30
	(6, 2)	3.67 (2.10)	−2.60	−0.43
Embedded-cluster	CP (2, 2, 2) *S*3	2.48	−1.65	−0.39
methods	(2, 2, 2) *S*5	3.32	−1.65	−0.39

Table 7. Binding energies E_B (eV), equilibrium distances R_e (au), and charge transfers Δn for the on-top site in the H/Li(100) system. The same conventions apply as for table 5.

On top		E_B (eV)	R_e (au)	Δn
	This work	1.8	3.3	−0.22
Cluster methods	BK (5, 4)	1.31 (1.55)	3.3	—
	(5, 4, 1)	0.54 (0.76)	3.3	—
	HR (4, 0)	1.36 (1.96)	3.3	−0.20
	(4, 5)	1.36 (0.24)	3.5	−0.20
Embedded-cluster	CP (5, 4, 1) *S*3	2.34	3.0	−0.52
methods	(5, 4, 1) *S*5	2.56	3.0	−0.52
	MLEC Li_{14}	0.86	3.14	0.23
	Li_{18}	1.52	3.14	0.15

In figure 4 our results for the interaction energy versus distance are presented. By contrast to the case for the method of CP, we observe that our results have the correct behaviour at the dissociation limit. On the other hand, it can also be seen that, contrary to the case for the on-top and on-centre positions, the results for the on-bridge position do not present a pronounced repulsive barrier, allowing for the possibility of H diffusion into the bulk of the solid. This result qualitatively coincides with the CP one. For the on-centre and on-top positions, the repulsive barrier arises from the proximity of the H to a particular Li atom. The equilibrium distance for the on-centre position is smaller, because the Li atom in front of the H is in the second layer.

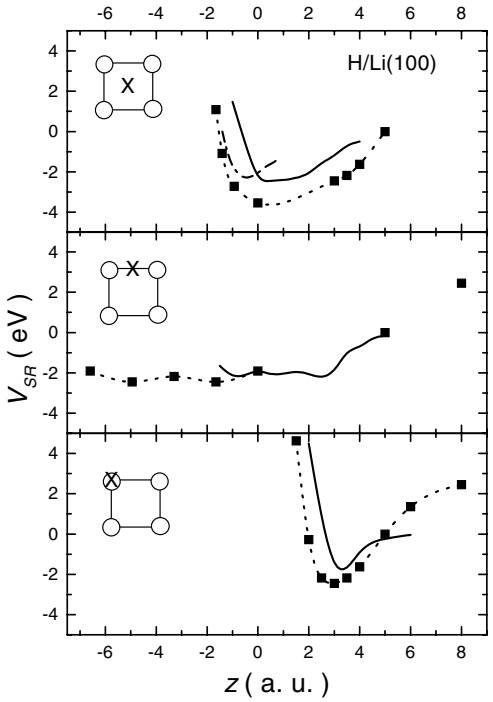

Figure 4. The interaction energy for H/Li(100) for on-centre, on-bridge, and on-top sites. ——: present work; · · · · · ·: reference [9]; — · —: reference [23].

3.2. Physisorption of He on Al and Na

Here, we will start with the calculation of $V_{SR}(z)$ for He/Al(111) and He/Na(110) systems. As can be seen in figures 5 and 6, our calculations include normal atom–surface separations from $z = 1$ au up to $z = 11$ au ($z = 0$ is defined as the plane of the superficial ions). Consequently, the resulting energies lie within an ample range covering five orders of magnitude. The calculated points were fitted with a Molliere-like potential and in both figures our results are compared with the exponential decay proposed in reference [18]. The inset includes the region relevant to physisorption. These figures also include an exponential-decay-like fitting of our results for $z \geqslant 5$ au. Good agreement between the results from the two calculations is found, particularly in the He/Al case. The more pronounced differences in the He/Na case may be due to the differences between the densities of states adopted for the two calculations. In reference [18] a renormalized Lang–Kohn (LK) surface barrier, expected to provide reasonably

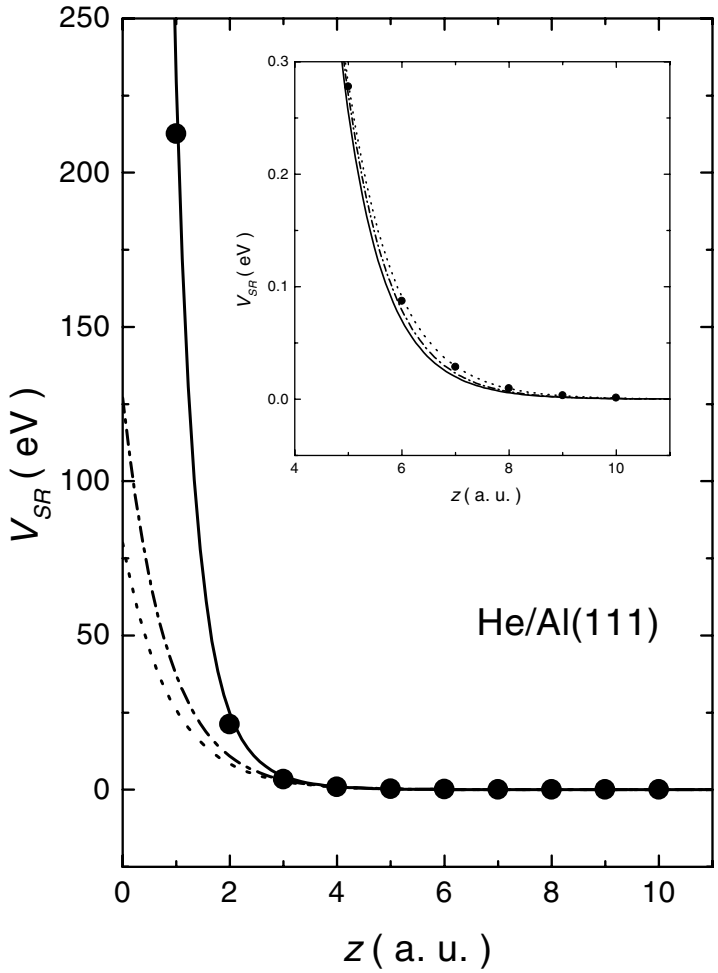

Figure 5. The repulsive potential for the He/Al(111) system. Dots: calculated points; ——: Molliere-like fitting: $V_{SR}(z) = (710/z)[0.43\exp(-1.1z)+1.47\exp(-2.1z)]$; · · · · · ·: exponential-decay fitting: $V_{SR}(z) = 6.58\exp[-1.13(z - 2.21)]$; — · —: reference [18]: $V_{SR}(z) = 8.38\exp[-1.23(z - 2.21)]$.

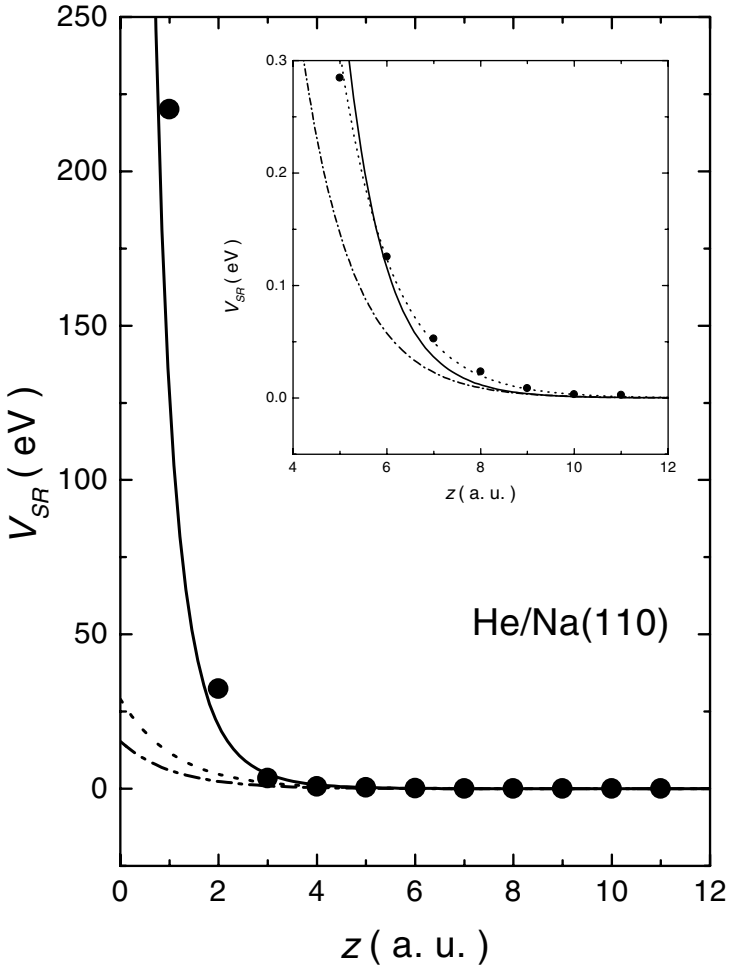

Figure 6. The repulsive potential for the He/Na(110) system. Dots: calculated points; ——: Molliere-like fitting: $V_{SR}(z) = (80/z)[3.5\exp(-z) + 2.5\exp(-2.1z)]$; · · · · · ·: exponential-decay fitting: $V_{SR}(z) = 2.15\exp[-0.91(z - 2.86)]$; — · —: reference [18]: $V_{SR}(z) = 1.07\exp[-0.93(z - 2.86)]$.

accurate densities of states particularly for metals with pronounced jellium-like character, was used. However, the results of reference [18] are very sensitive to changes in the LK surface barriers at positions close to the surface. By contrast, we have resorted to a LCAO expansion of the solid states that emphasizes the localized nature of the atom–atom interactions, adopting a semi-elliptical energy function to describe the partial and local densities of states. Thus, our model calculation tends to account properly for contributions due to short-range effects. These are related to the strong hybridizations among the states of the surface atoms with those on the physisorbed species occurring at positions close to the surface ($\lesssim$3 au). In order to evaluate how this prescription works in obtaining $V_{SR}(z)$, we will make the following comparisons:

(i) With a fixed van der Waals potential, we compare our repulsive contribution to the interaction energy with those obtained by ZK [2] and by Nordlander and Harris [18] (figure 7).

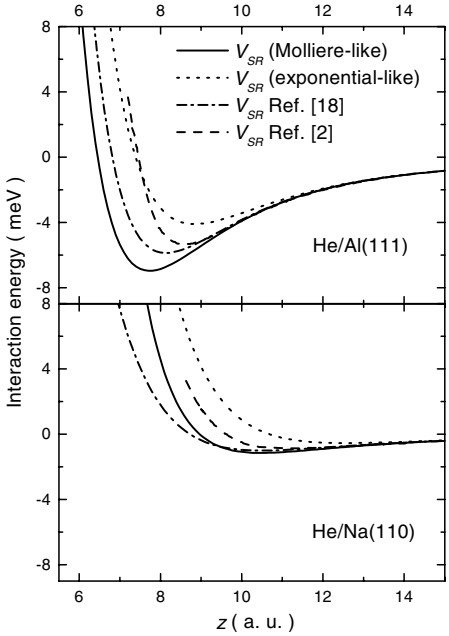

Figure 7. Physisorption potentials for different repulsive contributions. ——: Molliere-like fitting for V_{SR}; · · · · · ·: exponential-decay fitting for V_{SR}; - - - -: reference [2]; — · —: reference [18]. In all cases we use the van der Waals contribution from reference [2].

(ii) By using our results for $V_{SR}(z)$, we compare the effects of several van der Waals potentials on the atom–surface interaction energy (figure 8).

(iii) In figure 9 we analyse the changes in the interaction energies for different crystalline faces.

Figure 7 shows the changes introduced by the bond-pair model based on a localized–extended mixed picture of the atom–surface interaction when compared with results obtained under the jellium-like picture. These changes affect mainly the depth of the potential well and the location of the repulsive barrier with respect to the surface. With respect to the interaction energy, one observes that the uncertainties introduced by the different van der Waals potentials selected ($\Delta E \cong 3.6$ meV for He/Al) may even be much larger than those caused by the differences in the repulsive potentials ($\Delta E \cong 1.8$ meV for He/Al). As our calculation of $V_{SR}(z)$ has been performed by considering just the on-top position for the helium atom and includes only the interaction with its nearest neighbour at the surface, our results do not depend on the details of the atomic arrangement that corresponds to a particular crystalline face. The only dependence of the interaction energy on the crystalline face comes from the necessity of adopting a common origin for the two contributions $V_{SR}(z)$ and $V_{vdW}(z)$. This common origin is chosen as the plane defined by the surface ions. This requires one to define first the location of the plane surface ions corresponding to the different crystalline faces and the distance Z_{je} to the jellium edge, from which the van der Waals potential is measured (see table 1). The variations introduced in this form for different crystalline faces are not negligible, as shown in figure 9. Changes of 2.1 meV in the binding energy and 0.5 au in the equilibrium distance are obtained when going from the (100) to the (111) face of Al. For Na these same magnitudes show changes of 0.4 meV and 0.8 au between the (100) and the (110) faces.

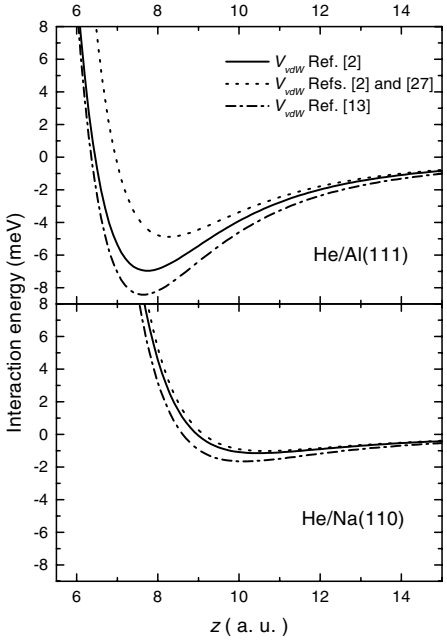

Figure 8. Physisorption potentials for different van der Waals contributions. ——: V_{vdW} from reference [2]; · · · · · ·: V_{vdW} from references [2] and [27]; — · —: V_{vdW} from reference [13]. In all cases we use the Molliere-like fitting for V_{SR}.

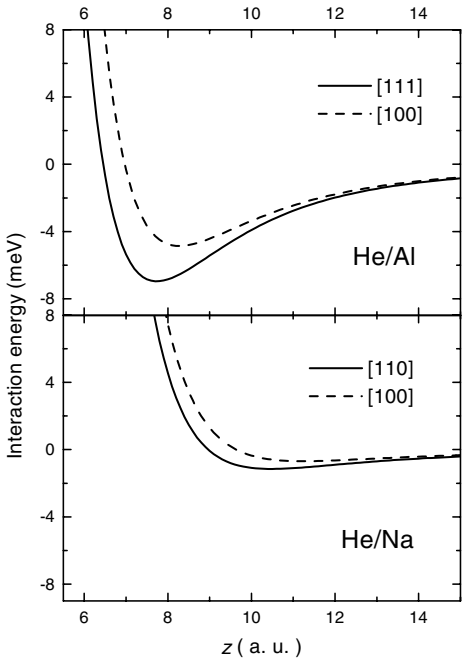

Figure 9. Physisorption potentials for different crystalline faces. In all cases we use the Molliere-like fitting for V_{SR} and V_{vdW} from reference [2].

4. Conclusions

By adopting a common basis to model the short-range contributions to the interaction energy of an adatom–surface system, we have examined the ability of our form to describe both the chemisorption and the repulsive contribution to the physisorption processes. The model calculation is based on an extended version of the Anderson (or Anderson–Newns) Hamiltonian under the bond-pair picture that includes, on *ab initio* grounds, the extended and the localized ingredients of the atom–surface interaction. When solved within the HF approximation, our results for chemisorbed H on Al and Li surfaces compare fairly well with those from other theoretical treatments obtained within DFT and cluster descriptions of the surface. In the case of He physisorbed on Al and Na surfaces, our results for the repulsive contribution to the interaction energy are also in good agreement with other theoretical calculations based on a jellium model description of the surface. On the other hand, as our model allows one to estimate this contribution on an *ab initio* basis, it could be used for applications to anomalous systems in which the anticorrugation phenomenon has been observed.

Acknowledgments

Financial support from Consejo Nacional de Investigaciones Científicas y Técnicas (CONICET) and Universidad Nacional del Litoral (UNL), Argentina, through grants PIP-4800/97 and CAI+D 94-E12, respectively, are gratefully acknowledged. One of us (PGB) wishes to acknowledge the partial financial support received from FOMEC No 331 (UNL) and Centro Atómico Bariloche.

References

[1] Lundqvist B I 1990 *Theoretical Aspects of Adsorption in Interaction of Atoms and Molecules with Solid Surfaces* ed V Bortolani, N H March and M P Tosi (New York: Plenum)
[2] Zaremba E and Kohn W 1977 *Phys. Rev.* B **15** 1769
Zaremba E and Kohn W 1976 *Phys. Rev.* B **13** 2270
[3] Hohenberg P and Kohn W 1964 *Phys. Rev.* **136** B864
Kohn W and Sham L J 1965 *Phys. Rev.* **140** A1133
[4] Gunnarsson O and Lundqvist B I 1976 *Phys. Rev.* B **13** 4274
[5] Perdew J P, Chevary J A, Vosko S H, Jackson K A, Pederson M P, Singh D J and Fiolhais C 1992 *Phys. Rev.* B **46** 6671
Perdew J P, Burke K and Ernzerhof M 1996 *Phys. Rev. Lett.* **77** 3865
[6] Beckman H O and Koutecky J 1982 *Surf. Sci.* **120** 127
Pacchioni G, Koutecky J and Beckmann H O 1984 *Surf. Sci.* **144** 602
[7] Ray A K and Hira A S 1988 *Phys. Rev.* B **37** 9943
Hira A S and Ray A K 1989 *Phys. Rev.* B **40** 3507
Hira A S and Ray A K 1990 *Surf. Sci.* **234** 397
Hira A S and Ray A K 1991 *Surf. Sci.* **249** 199
[8] Bonacic-Koutecky V, Gaus J, Guest M F, Cespiva L and Koutecky J 1993 *Chem. Phys. Lett.* **206** 528
[9] Casassa S and Pisani C 1995 *Phys. Rev.* B **51** 7805
[10] Krüger S and Rösch N 1994 *J. Phys.: Condens. Matter* **6** 8149
[11] Birkenheuer U, Boettger J C and Rösch N 1995 *Surf. Sci.* **341** 103
[12] Anderson Y, Langreth D C and Lundqvist B I 1996 *Phys. Rev. Lett.* **76** 102
[13] Hult E, Andersson Y and Lundqvist B I 1996 *Phys. Rev. Lett.* **77** 2029
[14] Kohn W, Meir Y and Makarov D E 1998 *Phys. Rev. Lett.* **80** 4153
[15] Edsberg N and Nørskov J K 1980 *Phys. Rev. Lett.* **45** 807
Nørskov J K and Lang N D 1980 *Phys. Rev.* B **21** 2131
[16] Rieder K H and García N 1982 *Phys. Rev. Lett.* **49** 43
Rieder K H, Parschau G and Burg B 1993 *Phys. Rev. Lett.* **71** 1059

[17] Petersen M, Wilke S, Ruggerone P, Kohler B and Scheffler M 1996 *Phys. Rev. Lett.* **76** 995
[18] Nordlander P and Harris J 1982 *J. Phys. C: Solid State Phys.* **17** 1141
[19] Harris J and Liebsch A 1982 *J. Phys. C: Solid State Phys.* **15** 2275
Harris J and Liebsch A 1982 *Phys. Rev. Lett.* **49** 341
[20] Bolcatto P G, Goldberg E C and Passeggi M C G 1998 *Phys. Rev.* B **58** 5007
[21] Hjelmberg H 1979 *Surf. Sci.* **81** 539
[22] Stumpf R 1997 *Phys. Rev. Lett.* **78** 4454
[23] García-Vidal F J, Martín-Rodero A, Flores F, Ortega J and Pérez R 1991 *Phys. Rev.* B **44** 11 412
[24] Paul J 1988 *Phys. Rev.* B **37** 6164
[25] Birkenheuer U, Boettger J C and Rösch N 1994 *J. Chem. Phys.* **100** 6824
[26] Bolcatto P G, Goldberg E C, Passeggi M C G and Flores F 1994 *An. AFA* **6** 4
[27] Liebsch A 1986 *Phys. Rev.* B **33** 7249